Rockbursts and Seismicity in Mines, Young (ed.) © 1993 Balkema, Rotterdam, ISBN 90 5410 320 5

Seismic attenuation in deep-level mines

S.M.Spottiswoode
Chamber of Mines Research Organisation of South Africa, Johannesburg, South Africa

ABSTRACT: P- and S-wave spectra from three deep-level gold mines and one platinum mine in South Africa were found to be well described by the f^{-2} model with attenuation (Q). Q was found to vary widely, from 20 for ray-paths through highly fractured ground to 1000 through solid rock, necessitating independent determination of Q for each phase. I was able to determine spectral fits for moment, corner frequency and f_{max} (Hanks 1982), even for low values of f_{max} less than the corner frequency. Under these conditions of "negative bandwidth", in excess of 98 percent of the radiated energy was lost to attenuation and peak velocity and acceleration were reduced by an order of magnitude. Stress drops ranged between 0.5 and 5 MPa and were independent of moment for moment values in the range of 10^8 to 10^{13} N-m.

1 INTRODUCTION

One of the requirements of modern mine seismic systems is the ability to provide accurate and reliable estimates of source parameters, typically moment and stress. Seismic moment estimates are important for quantitative studies of mine seismicity and relate to the problem of mining sequences and layouts and the resulting seismic deformations (Spottiswoode 1990). Stress drops drive the near-field ground velocities and are therefore directly relevant to the rockburst problem. In addition, Stewart and Spottiswoode (1993) found that times during which small events have higher stress drops than normal are more likely to be followed by seismic events with magnitude M>0. This report addresses the seismological problems of rock-mass attenuation on amplitudes and on the interpretation of body-wave spectra.

A number of authors, including Spottiswoode (1984), have characterized the high-frequency body-wave displacement spectral fall-off by assuming a value for Q and modelling the frequencies above the corner frequency ($f>f_0$) as $f^{-\gamma}$ where $\gamma \geq 2$. However, Hanks (1982), Hanks and McGuire (1981) and many other authors have argued for a flat acceleration spectrum above the corner frequency, and therefore for $\gamma = 2$, out to some maximum value, f_{max}, beyond which the spectrum crashes, or falls off more rapidly. More recently, a number of authors (e.g. Rebollar et al 1990) have described the high-frequency spectra by f^{-2} with frequency-independent Q. In this paper, this behaviour is written as:

$$\bar{A}(f) = \frac{\bar{A}(0)\exp(-\kappa f)}{1+(f/f_0)^2} \qquad (1)$$

with kappa (κ) described by:

$$\kappa = \kappa_0 + \frac{\pi R}{QV_c} \qquad (2)$$

where
$\bar{A}(f)$ is the displacement spectral density,
$\bar{A}(0)$ is the spectral plateau,
f_0 is the corner frequency,
R is the hypocentral distance,
Q is the quality (attenuation) factor,
κ_0 is attenuation attributed to near-source or near-geophone effects, in addition to the the effect of Q in the unfractured rock-mass, and
V_c is the phase velocity (for P or S waves).

Hank's (1982) f_{max} can be defined as:

$$f_{max} = 1/\kappa \qquad (3)$$

Churcher (1990) showed that ray-paths that avoid the stope and its associated region of fractured rock result in impulsive waveforms with little attenuation ($Q \approx 200$). Ray-paths that traversed the stope region were much more attenuated ($Q \approx 20$) and had a more complex appearance. Clearly, we cannot use a single value of Q for all ray-paths within a mine seismic network.

Analysis of small earthquakes is hampered by attenuation, and a wide bandwidth ($f_{max} - f_0 \gg 0$) is usually required for source mechanism studies (Hanks 1982 and McGarr 1984). This can be achieved either by studying only the larger events or by installing geophones closer to the source. As we do not wish to restrict mechanism studies only to the larger events, there is a need to work with bandwidths as small as possible.

In this paper, I report on the results of applying equation (1) to data from networks at several deep-level gold mines and one platinum mine, covering a range of mining conditions. The resulting attenuation has a profound effect on radiated energy and peak ground motion parameters. I will show that it is possible to invert for source parameters even for small events, even for phases having a "negative" bandwidth, defined as

$f_{max} - f_0 < 0$. Under these conditions, we record very little of the total radiated energy.

2 METHOD

I developed an algorithm (SOURCEQ) that automatically selected time windows, calculated spectra and performed the three-parameter fit for $\bar{A}(0)$, f_0 and κ to each spectrum, according to equation 1. SOURCEQ was used either in graphics mode to display the interpretation for each individual seismogram or in batch mode to process any number of events at a time, as follows.

Windows were automatically selected to cover both the P and S pulses, based on previously picked arrival times, as well as noise preceding the P-wave arrival. A cosine taper was applied at the beginning and end of each window. Windows that were too short or had poor signal-to-noise performance were rejected. Three-point smoothing was applied to the power spectra of the body waves and further smoothing to the noise spectra so that the range of frequencies with good signal-to-noise ratio could be identified automatically.

Initial values of $\bar{A}(0)$ and f_0 were obtained from the peak in the velocity spectrum, corrected by a user-selected value for κ. My algorithm for fitting equation (1) to the observed spectra improved on these initial values as follows:

1. A least-squares procedure was used to find $\bar{A}(0)$ and f_0 by minimizing the sum of the squares of the difference between the theoretical velocity spectrum and the observed velocity spectrum, corrected by the current value of κ. The least-squares procedure ensured that the radiated energy of the observed spectra was equal to the energy of the fitted spectra.

2. A new value of κ was then found from the slope of log {observed spectrum / theoretical spectrum} as a function of frequency.

These two steps were repeated until satisfactory convergence occurred. Calculations for each phase took about 0.2s on a 50MHz 486 PC.

As the effect of both κ and f_0 is a rapid fall-off in the spectral energy at high frequencies, inversion is fundamentally difficult for $\kappa f_0 \geq 1$. In addition, the shape of the spectrum at $f \approx f_0$ in equation 1 does not have a strong physical basis. These effects resulted in the inversion often failing for $\kappa f_0 \geq 1$, despite many attempts to stabilize the interaction between stages 1 and 2 by changing the inversion method. As seismologists usually select for source mechanism or ground motion studies only those seismograms for which $\kappa f_0 \ll 1$ (e.g. McGarr 1984), any analysis that relaxes this condition provides additional opportunities.

3 DATA SETS

Data for detailed analysis were selected from networks at three deep-level gold mines and one platinum mine, covering a range of mining conditions. The gold mine networks used COMRO's Portable Seismic System (Pattrick et al 1990), with geophones grouted at the ends of holes drilled some 3 to 10m out of access tunnels. The platinum data were recorded by a GENTEL system developed by General Mining (More O'Ferral et al, pers comm 1992).

Sampling rates varied from 1000 to 20 000 samples per second, depending on the network extent. Seismograms from SENSOR 4.5Hz or 14Hz geophones were amplified with a gain factor of 100 and digitized with a 12-bit 10V analogue-to-digital converter (Pattrick et al 1990). Peak velocity values were greater than 0.02 mm/s for all events: smaller events were usually rejected at the mine. Only a small sample of the recorded data for mines A, B and C were studied, obtained at random on previous visits to the mines.

Here follows a brief description of each network.

3.1 *Mine A*

The seismic network was installed to monitor seismicity around longwalls and stabilizing pillars in a mine in the East Rand. Eight geophones were placed in follow-behind off-reef drives, usually 25m in the foot-wall, across a region some 3km in extent at depths of 2~3km below surface.

3.2 *Mine B*

This network was installed to study scattered mining and remnant removal in a region with seismogenic faults and dykes in the Orange Free State mining district at depths of 2~3km below surface. 16 geophones covered a region 800m across and were placed in haulages some 80m below reef.

3.3 *Mine C*

This project was a test site within a shaft pillar and was aimed at investigating the fracturing around two 3m by 3m experimental drifts which were spaced 7m apart skin-to-skin, mined in a field stress of about 100MPa. Geophones were placed at the ends of 10m holes some 40m behind the advancing drifts. Most of the recorded events were associated with the development blasts and care was taken to exclude these events from this study.

3.4 *Mine D*

This system consisted of one set of triaxial geophones installed at the bottom of a 40m vertical borehole drilled from surface. The data presented here originate from platinum mining where the tabular excavations were supported with a system of regional and crush pillars at a depth of 750m to 1km below surface.

As surface reflections closely followed the direct wave, it was necessary to adjust the theoretical spectral shape by the reflected waves, P, SV and SH, allowing for their appropriate amplitudes (Aki and Richards 1980). SV waves outside the shear-wave window

were excluded from the analysis to avoid the associated surface waves.

In addition to the four primary data sets, I used some results from an off-reef site some 100m behind a highly stressed longwall in the Carletonville area (Hemp and Goldbach 1993) and from a study of mechanisms and ground motions by McGarr (1984).

4 ANALYSIS

In this section I will firstly justify the use of equation (1) using two events: figure 1 for a seismogram from mine A and figure 2 for mine B. As the conventional amplitude spectrum simply falls off sharply above either f_0 or f_{max}, the spectra were plotted as acceleration spectra. The acceleration spectral values were plotted as a function of log (frequency) to show the flat spectrum between f_0 and f_{max}, particularly for figure 2b, followed by a curved spectral fall-off for $f \geq f_{max}$. This curved region transforms to a linear fall-off in the log-linear plots in figures 2c and 2c, in clear agreement with

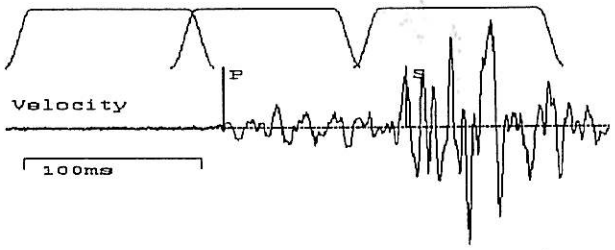

Figure 1a. A velocity seismogram for mine A, with windows marked for noise, P and S waves.

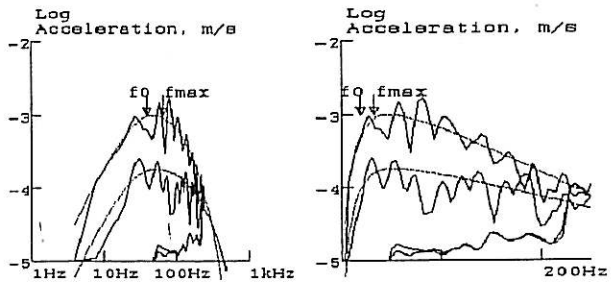

Figures 1b & c. From top to bottom: S, P and noise acceleration spectra from figure 1a. The fitted theoretical spectra as derived from equation 1 are the dotted, smooth curves. The derived values of f_0 and f_{max} are marked for the S-wave spectrum.

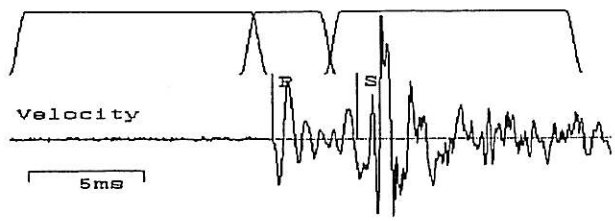

Figure 2a. Seismogram for mine B, as for figure 1a.

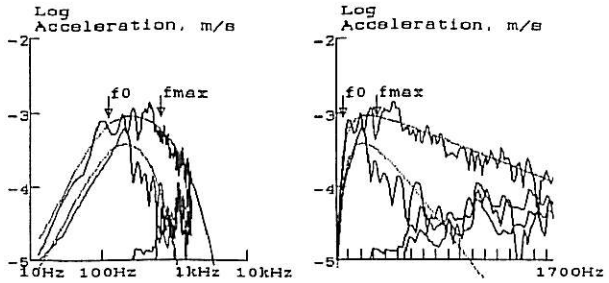

Figures 2b & 2c. As for 1b & 1c, derived from the seismogram in figure 2a.

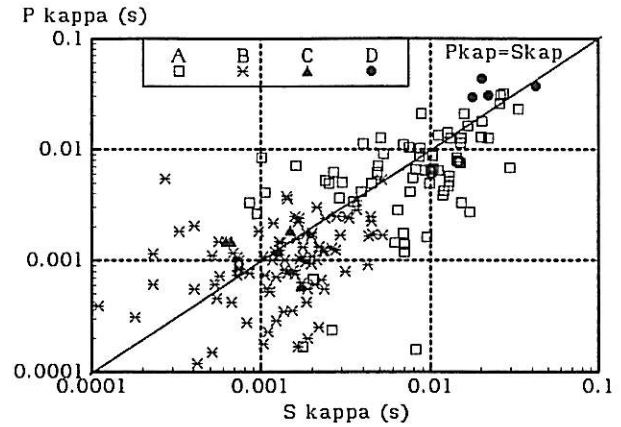

Figure 3. Attenuation as measured from P waves at different geophone sites compared to attenuation as measured from S waves. Data from the four mine sites are identified by the symbols in the box, as with the following figures.

frequency-independent attenuation (Q) from equations 1 and 2.

In figure 3 we can see that κ is approximately the same for P and S waves, and therefore $Q_P/Q_S \approx V_S/V_P$. The increased scatter for small values of κ for mines A and B is an effect generated by the log scale from errors in measurement.

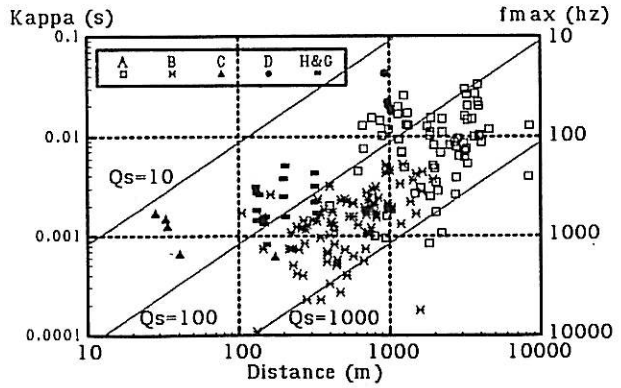

Figure 4. Attenuation (κ) as measured from S waves at different geophone sites for each mine as a function of hypocentral distance, R. Lines of constant Q are drawn for reference. In addition, data studied by Hemp and Goldbach (1993) were included, marked "H&G".

In figure 4, we can see that Q varies from about 20 to a fairly well-defined upper limit of 1000. The pattern of values on this plot for each data set showed considerable detail.

The values of kappa for mine A were bounded by two lines: a maximum value of κ of about 0.03s and a maximum value for Q of 1000. The maximum value of κ_0 is apparent for hypocentral distances varying from 1000m to 4000m. From equation 2, we can say that $\kappa_0 \leq 0.02$s and Q = 1000. The high value of $\kappa_0 = 0.02$s, or $f_{max} = 50$Hz, could be ascribed to the extensive fracturing around the large stope spans that were generated by the longwall mining.

Attenuation for mine B could be well described by Q = 200 to 1000, with little evidence for the existence of κ_0, in contrast to mine A. This could be attributed to smaller spans, better geophone positioning (further from reef) and the role of faults in drawing seismicity away from the highly fractured region around the stope faces.

Events for mine C were strongly grouped at $R \approx 40$m and $\kappa \approx 0.001$s. This was not surprising given the small range in ray-paths, and is good confirmation of the accuracy of the inversion procedure, given the range of moments for these events. The strong attenuation can be ascribed to the intense fracturing around the drifts, particularly since the events located near the drift ends and the rays travelled back along paths in the vicinity of the drifts.

The value of κ for mine D, 0.02s to 0.04s, or f_{max} = 25Hz to 50Hz, is in good agreement with values of f_{max} reported by Hanks (1982) for seismograms written at surface stations.

The low values of Q (Q<20) for the events studied by Hemp and Goldbach (1993) again illustrated high attenuation in the region around the stopes.

Static stress drops (τ) were calculated from Brune (1970):

$$\tau = \frac{7M_0}{16r_0^3} \qquad (4)$$

where:
M_0 is the seismic moment and

$$r_0 = \frac{2.34V_t}{2\pi f_0}$$

is the source radius as inferred from Brune (1970). In figure 5, we can see that the data studied here were compatible with previous mine seismic data (McGarr 1984). The stress drop was independent of event size over five orders of magnitude in moment.

5 EFFECT OF ATTENUATION ON SEISMOGRAMS

The radiated seismic energy of mine tremors is usually estimated by integrating the square of velocity over time, averaged over a number of geophones, assuming geometric spreading:

$$E = k\int v^2 dt \qquad (5)$$

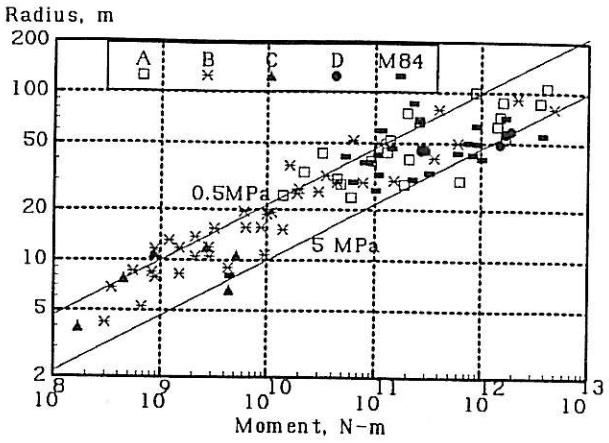

Figure 5. Source dimension as a function of seismic moment. Data marked as "M84" are mining events from McGarr (1984).

where k is a constant. From Parceval's theorem, the integration can be performed in the frequency domain, giving:

$$E = k\int \dot{v}^2 df \qquad (6)$$

and from equation 1,

$$E = k\tilde{A}(0)^2 \int \frac{f^2 \exp(-2.\kappa.f)}{(1+(f/f_0^2))^2} df \qquad (7)$$

For integration from zero to infinity, and substituting f for f/f_0, equation 7 reduces to:

$$E = kf_0^2\tilde{A}(0)^2 \int \frac{f^2 \exp(-2.\kappa.f_0.f)}{(1+f^2)^2} df \qquad (8)$$

Numerical integration is necessary for evaluating equation 8. The results are presented in figure 6, which shows the radical effect of small or "negative" bandwidth provided by $f_{max} < f_0$. Even for $\kappa f_0 = 0.2$ (or $f_{max} = 5f_0$), more than 50 percent of the radiated energy is lost to attenuation.

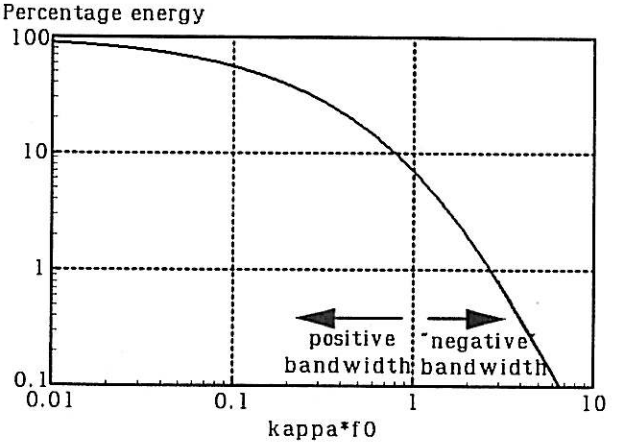

Figure 6. The effect of f0*kappa on recorded energy.

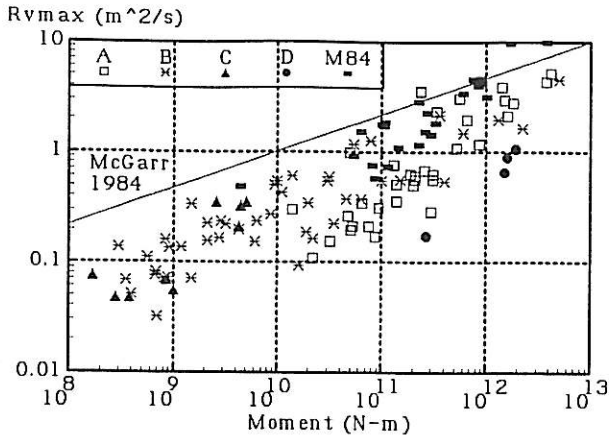

Figure 7. Hypocentral distance times peak velocity (Rv_{max}) as a function of seismic moment. An empirical relationship from McGarr(1984) for a depth of 2.5km is drawn for comparison.

We can see in figure 7 that the relationship of McGarr (1984) is a poor fit to the data. The fit for each data set is even worse for smaller values of M_0 than for larger values, for reasons that will become apparent.

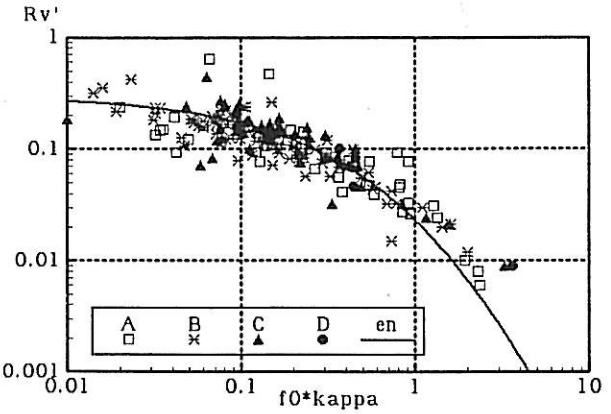

Figure 8. $Rv' = Rv_{max}/(\tau r_0)$, in arbitrary units, as a function of $f_0\kappa$. The energy attenuation curve from equation 8 and figure 6 is also plotted for comparison.

The peak velocity should be proportional to the product of stress drop and source radius (e.g. McGarr 1984). In figure 8, $Rv' = Rv_{max}/(\tau r_0)$ is compared to $f_0\kappa$ for individual seismograms. There is a very strong decrease in peak velocity with increasing values of $f_0\kappa$, in close agreement with the theoretical decrease in energy. Figure 8 shows that the peak velocity can generally be estimated within a factor of two, given M_0, τ and $f_0\kappa$.

Similar analysis of the ground motion parameter $\rho R a_{max}$, where ρ is the density and a_{max} is the peak ground acceleration, showed a very similar trend to that shown for peak velocity in figure 8.

6 CONCLUSIONS

I have found that Q varies widely, from 20 for highly fractured ground to 1000 for long ray-paths through solid ground. These extreme variations make corrections for an assumed constant Q subject to large errors.

1. Source mechanism studies of small mine events are feasible only if spectra are simultaneously inverted for attenuation, κ.

2. Simultaneous inversion for M_0, f_0 and κ is possible, even for $f_0\kappa < 1$.

3. Attenuation has a profound effect on energy, peak velocity and peak acceleration.

Acknowledgement

This work forms part of the research program of the Chamber of Mines. Thanks to Dr W. Rymon-Lipinski, Ms D. Hemp, and Messrs P. Chetty, N. Cook, M. Grave, R. Kersten, D. Minney, R. More O'Ferral and M. Spengler for providing me with seismic data. Thanks also to Dr N.C. Gay and Mr R.D. Stewart for reviews and comments.

REFERENCES

Aki, K. & P.G. Richards 1980. *Quantitative seismology*. San Francisco : W.H. Freeman.

Brune, J.N. 1970. Tectonic stress and the spectra of seismic shear waves from earthquakes. *J. Geophys. Res.* 75: 4997-5009. (Correction. 1971, *J. Geophys. Res.* 76: 5002).

Churcher, J.M. 1990. The effect of propagation path on the measurement of seismic parameters. *Proceedings of the 2nd International Symposium on Rockbursts and Seismicity in Mines*: 205-209. Minnesota: Balkema.

Hemp, D.A. & O.D. Goldbach 1993. The effect of backfill on ground motion in a stope during seismic events. *Proceedings of the 3rd International Symposium on Rockbursts and Seismicity in Mines*: this issue. Kingston: Balkema.

Hanks, T.C. 1982. f_{max}, *Bull. Seism. Soc. Am.*, 72, 1867-1879.

Hanks, T.C. & R.K. McGuire 1981. The character of high-frequency ground motion. *Bull. Seism. Soc. Am.* 71: 2071-2095.

McGarr, A. 1984. Scaling of ground motion parameters, state of stress, and focal depth. *J. Geophys. Res.* 89: 6969-6979.

Pattrick, K.W., A.M. Kelly & S.M. Spottiswoode 1990. A portable seismic system for rockburst applications. *International Deep Mining Conference : Technical challenges in deep level mining*: 1133-1146. Johannesburg: SAIMM.

Rebollar, C.J., L. Munguía, A. Reyes, A. Uribe & O. Juménaz 1991. Estimates of shallow attenuation and apparent stresses from aftershocks of the Oaxaca earthquake of 1978. *Bull. Seism. Soc. Am.* 81: 99-108.

Spottiswoode, S.M. 1984. Source mechanisms of mine tremors at Blyvooruitzicht Gold Mine. *Proceedings of the First International Symposium on Rockbursts and Seismicity in Mines*: 29-37. Johannesburg, S. Afr. Inst. of Min. Metall.

Spottiswoode, S.M. 1990. Volume excess shear stress and cumulative seismic moments. *Proceedings of the Second International Symposium on Rockbursts and Seismicity in Mines*: 39-43. Rotterdam: Balkema.

Stewart, R.D. & S.M. Spottiswoode 1993. A technique for determining the seismic risk in deep-level mining. *Proceedings of the 3rd International Symposium on Rockbursts and Seismicity in Mines*: this issue. Kingston: Balkema.